

Cantilevered bimorph-based scanner for high speed atomic force microscopy with large scanning range

Yusheng Zhou, Guangyi Shang,^{a)} Wei Cai, and Jun-en Yao

Department of Applied Physics, Beihang University, Beijing 100191, People's Republic of China
and Key Laboratory of Micro-nano Measurement-Manipulation and Physics (Ministry of Education),
Beihang University, Beijing 100191, People's Republic of China

(Received 14 August 2009; accepted 20 April 2010; published online 27 May 2010)

A cantilevered bimorph-based resonance-mode scanner for high speed atomic force microscope (AFM) imaging is presented. The free end of the bimorph is used for mounting a sample stage and the other one of that is fixed on the top of a conventional single tube scanner. High speed scanning is realized with the bimorph-based scanner vibrating at resonant frequency driven by a sine wave voltage applied to one piezolayer of the bimorph, while slow scanning is performed by the tube scanner. The other piezolayer provides information on vibration amplitude and phase of the bimorph itself simultaneously, which is used for real-time data processing and image calibration. By adjusting the free length of the bimorph, the line scan rate can be preset ranging from several hundred hertz to several kilohertz, which would be beneficial for the observation of samples with different properties. Combined with a home-made AFM system and a commercially available data acquisition card, AFM images of various samples have been obtained, and as an example, images of the silicon grating taken at a line rate of 1.5 kHz with the scan size of 20 μm are given. By manually moving the sample of polished Al foil surface while scanning, the capability of dynamic imaging is demonstrated. © 2010 American Institute of Physics. [doi:10.1063/1.3428731]

I. INTRODUCTION

Since the atomic force microscope (AFM) was invented, it has been an important tool for research in nanoscience and nanotechnology.¹ If the speed of imaging could be increased to the video rate, AFM would be regarded as one of the most elegant techniques for monitoring dynamic process such as crystallization and biological process in nanometer scale as well as fast nanolithography.^{2–8} During the past decade, many efforts have been made in the technical areas including increasing lateral scanning speed,⁷ improving the algorithm of feedback in z -direction,⁹ designing new cantilever with smaller dimension,¹⁰ and so forth.

Lateral scanning is an important technique for any scanning probe microscopy (SPM) system. The history of SPM records many scanning devices such as tripod scanner, piezoelectric single tube scanner, and three independent piezoelectric actuators.¹¹ The highest scanning speed to be achieved is mainly determined by the dynamic behavior of the scanner. In the literature, two possible approaches to increase the scan speed can be found. One is to increase the resonance frequency of the scanner by designing it as small, light, and rigid as possible, and the other is realized by scanning at the resonance frequency of the scanner. Schitter *et al.*⁷ developed a high speed scanner based on a flexure mechanism and piezoelectric stack actuators, which is more rigid resulting in high resonant frequency. Combined with a shaped driven signal, the device can scan at 7800 lines/s. Ando *et al.*¹² also

designed a high speed scanner by mounting piezostacks on top of each other, achieving at line scan rate of 1.25 kHz. Rost *et al.*¹³ used shear-mode piezoelectric actuators in scanning tunneling microscope, which allows imaging speed up to 0.3 mm/s with scan range of 300 nm. In those designs, the scan speed is increased by increasing the first resonant frequency of the scanner. High power amplifiers are necessary to drive the piezostacks at high frequency and a significant issue of thermal dissipation should be taken into account when working for a long time. Scan range of this kind of scanners is limited to less than 15 μm .^{7,9,13} Humphris *et al.*¹⁴ and Picco *et al.*¹⁵ successfully used a tuning fork as a fast axis scanner, with which line scan rate of 20–100 kHz was reached. Compared with the piezostack-based scanners, the main advantage of the tuning fork scanner is the fact that it is simple in structure and does not need high power amplifier. However, since the dimensions of tuning fork are very small, it cast strict limitation on sample size (smaller than $1 \times 1 \text{ mm}^2$). Additionally, the equivalent mass should be mounted on the other leg of tuning fork to avoid undesired vibration of z -direction.

Recently, Yongho *et al.*¹⁶ developed a microscanner served as a fast-scan dimensional motion by combining a brass bar with a piezoactuator, which breaks the limitation on sample size. Compared with tuning fork scanner, however, this design needs an additional piezo to actuate and it cannot detect the vibration information including amplitude and phase lag simultaneously. The latter is important for real-time phase compensation and scan range calibration in the resonance scanning mode. In addition, both the tuning fork and the microscanners suffer from a small scan size, which

^{a)} Author to whom correspondence should be addressed. Electronic mail: gyshang@buaa.edu.cn.

TABLE I. Parameters of current high speed scanning approaches (tuning fork needs additional equivalent mass to counterbalance the sample weight, NA means there is no motion sensor to detect the lateral scanning motion in the scanner design).

	Highest line scan rate (kHz)	Sample size (mm ²)	Scan range (fast axis) (μm)	Driven power	Motion sensing	Average Tip-sample velocity (mm/s)	Reference
“Comb” flexure structure	~ 7	$\sim 2 \times 2$	~ 15	High voltage and current	Piezoresist sensing	~ 100	7, 10, and 11
Overlap of piezostacks	~ 3	$\sim 1 \times 1$	~ 1	High voltage and current	NA	~ 2	5, 9, and 12
Shear mode PZT	~ 10	$\sim 5 \times 5$	~ 1	High voltage	NA	~ 0.3	13
Tuning fork	~ 20 – 100	$\sim 1 \times 1$	~ 0.5 – 5	Low voltage	Current sensing	~ 200	14 and 15
Brass bar scanner	~ 5 – 10	Unlimited	1–3	Low voltage	NA	~ 10	16
Bimorph scanner	~ 1 – 10	$\sim 5 \times 5$	~ 20 – 40	Low voltage	Voltage sensing	~ 120	

limit the range of applications. For example, in the study of biological process such as cell adaptation, larger scan range is often preferred for monitoring dynamic behavior of cells.

In this paper, we present an alternative high speed scanning design, which consists of a cantilevered bimorph-based scanner and a single tube scanner. The free end of the bimorph is used for mounting a sample stage while the other end is fixed on top of the tube scanner. High speed scan is realized with the bimorph-based scanner vibrating at resonant frequency driven by a sine wave signal, while slow scanning is performed by the tube scanner. The tube scanner can also provide three dimensional motions, which is identical to that in the conventional AFM for imaging. Using a home-made AFM system and a commercially available data acquisition (DAQ) card, AFM images of various samples have been obtained at the rate of 15–25 frames per second with 100×100 pixels and the scan range of larger than $20 \mu\text{m}$ can be achieved. The results suggest that this cantilevered bimorph-based scanner is very easy to implement, compatible with a conventional AFM system and shows promising potential for biological and nanofabrication applications since it has a large scan range. We here summarize some critical parameters of current high speed scanning approaches for comparison with our design, as given in Table I.

II. EXPERIMENTAL SETUP

The bimorph-based scanner is schematically shown in Fig. 1. By means of a specially designed holder that basically has a pair of blocks (B, B') and a base plate (P), the bimorph consisting of two piezoelectric layers attached to a conductive middle shim is rigidly clamped at one of its ends, forming a cantilevered beam with dimensions of length l , width w , and thickness t . The longitudinal axis of the beam is parallel to the base plate. A small sample stage is fixed (with superglue) on the top side of the beam free end.

When designing the bimorph-based scanner, several parameters are important and need to be taken into account, including the spring constant k_0 , the resonant frequency f_0 , quality factor Q , and the displacement sensitivity to voltage at the free end of the bimorph S . For a homogeneous cantilever with uniform cross section, the spring constant k_0 and the resonant frequency f_0 are given by $k_0 = Ewt^3/4l^3$ and $f_0 = (\eta_0/2\pi)(t/l^2)(E/12\rho)^{1/2}$, respectively, where E is the Young's modulus, $\eta_0 = 1.875$, ρ is the mass density.¹⁷ For operation in the high speed mode, the middle electrode of the

bimorph is earthed. One of the piezolayers, serving as a driving piezo, is connected to an output of a D/A converter. When applying a constant sine wave voltage to the driving piezolayer, mechanical vibration of the bimorph takes place as a result of the antipiezoelectric effect. If the bimorph is driven at its resonant frequency, the vibrating bimorph allows the sample stage to scan at a high speed. The displacement sensitivity S could be approximately estimated by the formula $d_{31}(l/h)^2Q$, where h is the thickness of one piezolayer, d_{31} is piezoelectric strain coefficient, the quality factor Q is defined as $f_0/\Delta f$, and Δf is the full width at half maximum. The other piezolayer is used as a detection piezo, generating an induced piezovoltage based on the piezoelectric effect. The induced voltage can be used to monitor the vibration of the bimorph and the phase lag between the signals from the driving and detection piezolayers, respectively, for real-time phase compensation.

In our experiment, the bimorph beams were fabricated by cutting them from a commercially available piezobimorph wafer (Institute of Acoustics, Chinese Academy of Sciences). Based on the given parameters including the length l , thickness t , elastic modulus E , the density ρ , and piezoelectric coefficient d_{31} , several typical design values were calculated, as given in Table II. The Q -factors were experimentally obtained by measuring the bimorph vibration as a function of the frequency and making the Lorentzian fits to the data. The results in Table II indicate that the spring constant and resonant frequency can be designed, which has the advantage that (i) the spring constant can be chosen according to the properties of a sample to be observed such as size and weight, (ii) the resonant frequency can be determined according to the expected scan speed. As an example, the relationship between the resonance frequency and the geometric parameter (length) of the bimorph is shown in Fig. 2. When



FIG. 1. Schematic diagram of the cantilevered bimorph-based scanner for high speed scanning.

TABLE II. Summary of the typical design values for the bimorph-based scanner, calculated with parameters of width $w=1.44$ mm, thickness $t=0.8$ mm, $h=0.3$ mm, elastic modulus $E=5.2 \times 10^{10}$ N/m², the density $\rho=6500$ kg/m³, $d_{31}=1.71 \times 10^{-10}$ m/V. The Q -factors were experimentally obtained.

Length (mm)	Spring constant (N/m)	Resonance (kHz)	Sensitivity ($\mu\text{m}/\text{V}$)	Quality factor
9	13 148	2.40	3.61	19
12	5547	1.35	4.84	13
15	2840	0.86	6.16	10

both the spring constant and the resonance are defined, the sensitivity can be deduced and used to estimate the scan range.

A home-made AFM system working in the contact mode was prepared for demonstrating the possibility of the bimorph-based scanner operating in the high speed. As shown in Fig. 3, the bimorph-based scanner is fixed on top of the single tube scanner. The longitudinal axis of the bimorph is carefully aligned with the y -direction of the tube scanner, forming a hybrid scanning unit. Obviously, high speed scanning is realized with the bimorph beam vibrating on resonant frequency, while slow scan is performed by the tube scanner. The tube scanner can also provide motion in x - y -directions for scanning and in z -direction for keeping an average height of the sample surface when AFM imaging. The hybrid scanning unit is mounted on a micropositioning stage for sample movement. The laser beam deflection method is adopted to detect the motion of the AFM cantilever. For employing a small cantilever, an aspheric lens is introduced to focus the collimated laser beam on the cantilever with a spot of less than $20 \mu\text{m}$ in diameter.

A commercially available DAQ card (National Instruments, S6115PCI), having 4 A/D and 2 D/A converters, was employed in our experiment for real time data acquisition and processing. As described previously, one of the D/A converters is connected to the driving piezolayer of the bimorph for high speed scanning in x -direction while the other to the tube scanner for y -direction motion. The AFM deflection data are fed to an A/D converter, which is sampled synchronously with the scan signals. The piezovoltage induced by the detection layer of the bimorph is also input to another

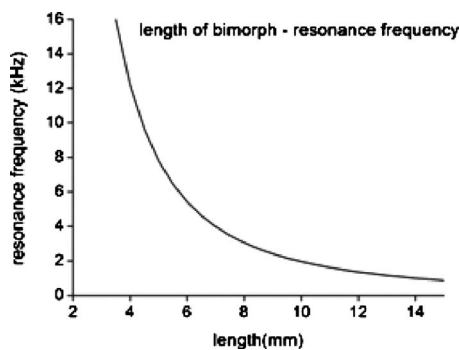


FIG. 2. Line scan rate (resonance frequency of the bimorph scanner) is a function of the length of the bimorph scanner.

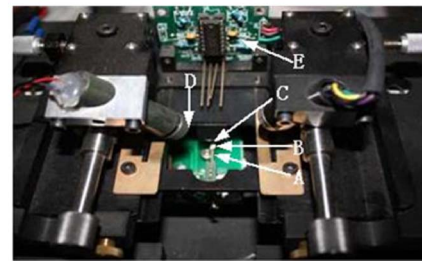
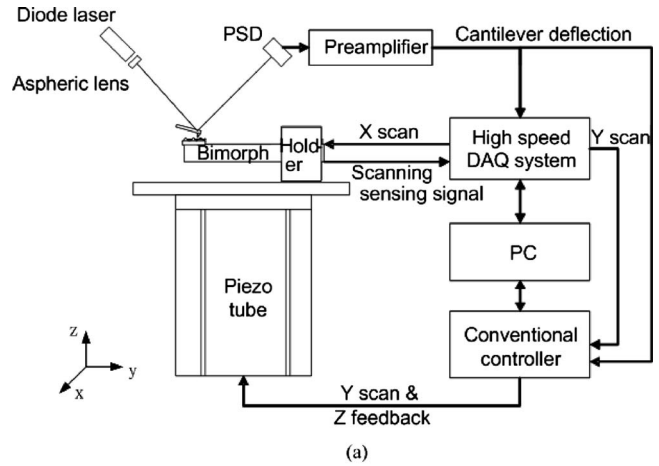


FIG. 3. (Color online) (a) Schematic structure of the high speed AFM system. The bimorph-based scanner is fixed on top of the tube scanner. Aspheric lens is used to focus the collimated laser beam on the cantilever with a small spot. (b) The home-made AFM head basically consisting of the bimorph-based scanner (a), the sample stage (b), AFM cantilever (c), the aspheric lens (d), and the preamplifier (e).

A/D converter, which provides information about the phase lag between the drive voltage signal and actual sample displacement.

A kind of commercially available cantilever, Bio-Lever mini (BL-AC40TS-C2, Olympus) with dimension of 0.1 N/m stiffness and resonant frequency of 110 kHz is employed for imaging in high speed mode.

III. EXPERIMENTS AND RESULTS

In the preliminary experiment, a calibrated silicon grating with a pitch of $10 \mu\text{m}$ as a test sample was observed with the AFM system. The sample has 5×5 mm² in size and was directly glued onto the free end of the bimorph. Since the high speed scan signal is sine wave around the resonant frequency of bimorph, the nonlinear motion of the sample together with phase lag between its motion and driving signal result in the distortion of images in the fast scan

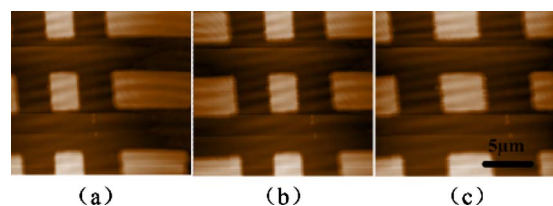


FIG. 4. (Color online) AFM images of a calibrated silicon grating as a test sample, showing that the image data can be amended in real time. The line scan rate was 1.5 kHz and each image took 67 ms with 100×100 pixels.

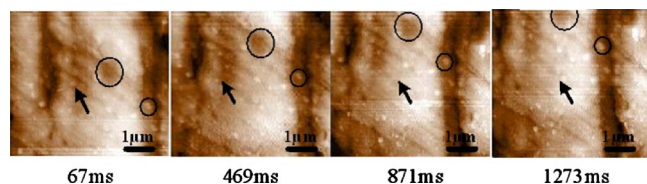


FIG. 5. (Color online) Four pictures of an Al surface, taken with the sample moving along the direction marked by the arrow. Every sixth image in the series is shown and each image was acquired in 67 ms.

axis. As shown in Fig. 4(a), the image contains the combination of part of scan forward and part of scan backward, since the collection start point is not identical to the end of the sample due to phase lag when sample is moved. Comparing the signal from the sensing electrode of the bimorph with scanning driving signal, the phase lag could be easily measured and compensated in real time by shifting certain number of collected data in each line corresponding to the degree of lagged phase. After phase lag compensation, as shown in Fig. 4(b), the grids near the center of the image are narrower than those in the edges of the image due to different scan speeds near the center of the image compared with the edges of the image. With an algorithm of interpolation,¹⁸ the data can be deconvoluted in real time, forming an image without any distortion as shown in Fig. 4(c). Benefited from the sensing electrode of the bimorph scanner, the image amendment was done in real time.

In addition, as indicated in Fig. 4(c), the lateral scan range is about 20 μm with a line scan rate of 1.5 kHz and the image was acquired in 67 ms with 100×100 pixels. In fact, the amplitude of driving signal in this experiment is less than 5 V, which indicates a potential of larger lateral scan range with a higher driving signal. This would be a unique feature of the bimorph scanner among those high speed scanner designs for large area imaging such as observing cell dynamic process in less than 0.1 s.

In our experiments, the actual scan range of the bimorph-based scanner was calibrated in the following way: (i) to take an image of a sample using the tube scanner and then measure the distance d_1 between two microfeatures along x -direction in the image, where d_1 is used as a reference value since the scan range of the tube scanner is precalibrated, (ii) to take an image of the same region of the sample using the bimorph-based scanner and measure the distance d_2 between the two same microfeatures, and (iii) by comparing d_1 with d_2 , the calibration of the bimorph-based scanner can be performed. In the further work, we should introduce an optical method such as interference to measure the scanning range of the bimorph-based scanner in real time.

In order to further show the capability of the AFM system, experiments on dynamic imaging were performed in such way that the sample being observed was moved by manually adjusting the micropositioning stage while imaging. Figure 5 displays four pictures cut from a series of images of the polished surface of a small Al foil taken in the contact mode, where some grooves and nanometer particles on the surface can be clearly seen. Since each image of 100×100 pixels was acquired in 67 ms, it is possible to

capture the images at a rate of 15 frames/s. By using a shorter bimorph beam, the rate of 25 frames/s can be easily obtained. In this case, the movement of the sample surface structures can be observed in real time, similar to what is available with a scanning electron microscope. Those results imply that the high speed AFM system could be used for studying the dynamic behavior of samples.

IV. DISCUSSION

In summary, we have successfully developed an alternative scanner for high speed AFM imaging. The main characteristic of the scanner is the use of a bimorph, in which one of piezolayers is employed to drive the sample to scan in a high speed and the other is done to monitor bimorph vibration. The significant advantage of the bimorph-based scanner with respect to the tuning fork is the fact that the spring constant and the resonant frequency of the bimorph can be designed and chosen, which would be beneficial for the observation of samples with different properties. Compared with the microscanner, the bimorph-based scanner has the capability of detecting the motion including amplitude and phase lag simultaneously. Based on the scanner, a high speed AFM system with a real time DAQ card has been built. AFM images of various samples were obtained at the rate of 15–25 frames per second with 100×100 pixels and the scan range of larger than 20 μm was achieved. The results suggest that the system is very reliable, repeatable, and easy to use.

In further work, we will develop a bimorph-based cantilever scanning device in place of the sample scanning one, which would provide a possible way to observe samples with larger dimensions or to operate in liquids. Those capabilities would be important for applications such as nanofabrication, surface modification, and biological phenomenon investigation.

ACKNOWLEDGMENTS

This work was supported by the National Natural Science Foundation of China (NSFC) (Grant No. 10827403) and the China National Key Basic Research Program (Grant No. 973, 2007CB936503).

- ¹G. Binnig, C. F. Quate, and C. Gerber, *Phys. Rev. Lett.* **56**, 930 (1986).
- ²R. C. Barrett and C. F. Quate, *J. Vac. Sci. Technol. B* **9**, 302 (1991).
- ³P. K. Hansma, G. Schitter, G. E. Fantner, and C. Prater, *Science* **27**, 314 (2006).
- ⁴T. Ando, T. Uchihashi, and T. Fukuma, *Prog. Surf. Sci.* **83**, 337 (2008).
- ⁵T. Fukuma, Y. Okazaki, N. Kodera, T. Uchihashi, and T. Ando, *Appl. Phys. Lett.* **92**, 243119 (2008).
- ⁶A. D. L. Humphris, J. K. Hobbs, and M. J. Miles, *Appl. Phys. Lett.* **83**, 6 (2003).
- ⁷G. Schitter, P. J. Thurner, and P. K. Hansma, *Mechatronics* **18**, 282 (2008).
- ⁸J. A. Vicary and M. J. Miles, *Nanotechnology* **20**, 095302 (2009).
- ⁹N. Kodera, H. Yamashita, and T. Ando, *Rev. Sci. Instrum.* **76**, 053708 (2005).
- ¹⁰G. Fantner, G. Schitter, J. Kindt, T. Ivanov, K. Ivanova, R. Patel, N. Holten-Andersen, J. Adam, P. J. Thurner, I. W. Rangelow, and P. K. Hansma, *Ultramicroscopy* **106**, 881 (2006).
- ¹¹G. Schitter, Proceedings of the American Control Conference, 2007, p. 3503.
- ¹²T. Ando, N. Kodera, E. Takai, D. Maruyama, K. Saito, and A. Toda, *Proc. Natl. Acad. Sci. U.S.A.* **98**, 12468 (2001).
- ¹³M. J. Rost, L. Crama, P. Schakel, E. van Tol, G. B. E. M.

- van Velzen-Williams, C. F. Overgaw, H. ter Horst, H. Dekker, B. Okhuijsen, M. Seynen, A. Vijftigschild, P. Han, A. J. Katan, K. Schoots, R. Schumm, W. van Loo, T. H. Oosterkamp, and J. W. M. Frenken, *Rev. Sci. Instrum.* **76**, 053710 (2005).
- ¹⁴A. D. L. Humphris, M. J. Miles, and J. K. Hobbs, *Appl. Phys. Lett.* **86**, 034106 (2005).
- ¹⁵L. M. Picco, L. Bozec, A. Ulcinas, D. J. Engledew, M. Antognozzi, M. A. Horton, and M. J. Miles, *Nanotechnology* **18**, 044030 (2007).
- ¹⁶Y. Seo, C. S. Choi, S. H. Han, and S. Han, *Rev. Sci. Instrum.* **79**, 103703 (2008).
- ¹⁷D. Sarid, *Scanning Force Microscopy* (Oxford University Press, Oxford, 1991), Chap. 1.
- ¹⁸Z. Li, Q. Li, X. Cheng, and Q. Wang, *Infrared and Laser Engineering* **34**, 146 (2005).